LASER INTERFEROMETER GRAVITATIONAL WAVE OBSERVATORY
- LIGO -
CALIFORNIA INSTITUTE OF TECHNOLOGY
MASSACHUSETTS INSTITUTE OF TECHNOLOGY

Technical Note **LIGO-T0900144-v1-D** Date: 2009/04/08

Adv. LIGO Arm Length Stabilisation Design

Peter Fritschel, David McClelland, Adam Mullavey, Daniel Shaddock, Bram Slagmolen, Sam Waldman, et. al

Distribution of this document:

Detector Group

Draft

California Institute of Technology
LIGO Project, MS 18-34
Pasadena, CA 91125
Phone (626) 395-2129
Fax (626) 304-9834
E-mail: info@ligo.caltech.edu

Massachusetts Institute of Technology
LIGO Project, Room NW17-161
Cambridge, MA 02139
Phone (617) 253-4824
Fax (617) 253-7014
E-mail: info@ligo.mit.edu

LIGO Hanford Observatory
Route 10, Mile Marker 2
Richland, WA 99352
Phone (509) 372-8106
Fax (509) 372-8137
E-mail: info@ligo.caltech.edu

LIGO Livingston Observatory
19100 LIGO Lane
Livingston, LA 70754
Phone (225) 686-3100
Fax (225) 686-7189
E-mail: info@ligo.caltech.edu

http://www.ligo.caltech.edu/

Contents

1 Introduction

The quadruple suspension system (quad) designed for the test masses, provide isolation of the ground motion to the test mass at frequencies above 10 Hz. Displacements at frequencies below and near the quadruple suspension resonance frequencies will not be well attenuated. Complex feedback will damp the suspension resonance modes. Even with the BSC ISI platforms, this results in the test mass displacement of $\sim 10^{-7}$ m/$\sqrt{\text{Hz}}$ below 0.5 Hz. This displacement is too much for the actuators mounted on the quad to acquire lock of the arm cavities in a deterministic manner. To make the lock acquisition more deterministic, the arm cavities are locked independently from the central recycling cavities. The independent arm locking scheme will enable to introduce a small offset of the cavity resonance with the main laser. The lock acquisition of the recycling cavities will then not be hindered by the arm cavities going through resonance and breaking the acquisition process. Once the recycling cavities have been locked, the offset on the arm cavities is reduced to bring them into resonance with the main laser.

To achieve the deterministic locking procedure, the residual arm cavity length fluctuations need to be reduced to within the line-width of the cavity, the line-width equivalent displacement is 1.3 nm.

This document describes the conceptual design for the Arm Length Stabilisation system.

2 Approach

The approach for stabilising the arm length fluctuations, is to use an auxiliary laser at 532 nm and inject it from the back of the arm cavity through the ETM. The laser frequency is locked to the arm cavity using the PDH technique. Once locked, feedback to the laser frequency keeps the error signal in its linear range, so the error signal can be fed back to the ITM/ETM to reduce the test mass displacement.

The HR coatings on the ITM and ETM will be modified to provide a chosen reflectivity for the 532 nm beam. The ITM will have a higher reflector then the ETM, resulting in an overcoupled cavity for the 532 nm beam.

3 Requirements

The requirements are described in T0900095, of which the main displacement requirement is shown in figure 1.

In table 1 various system requirements are repeated.

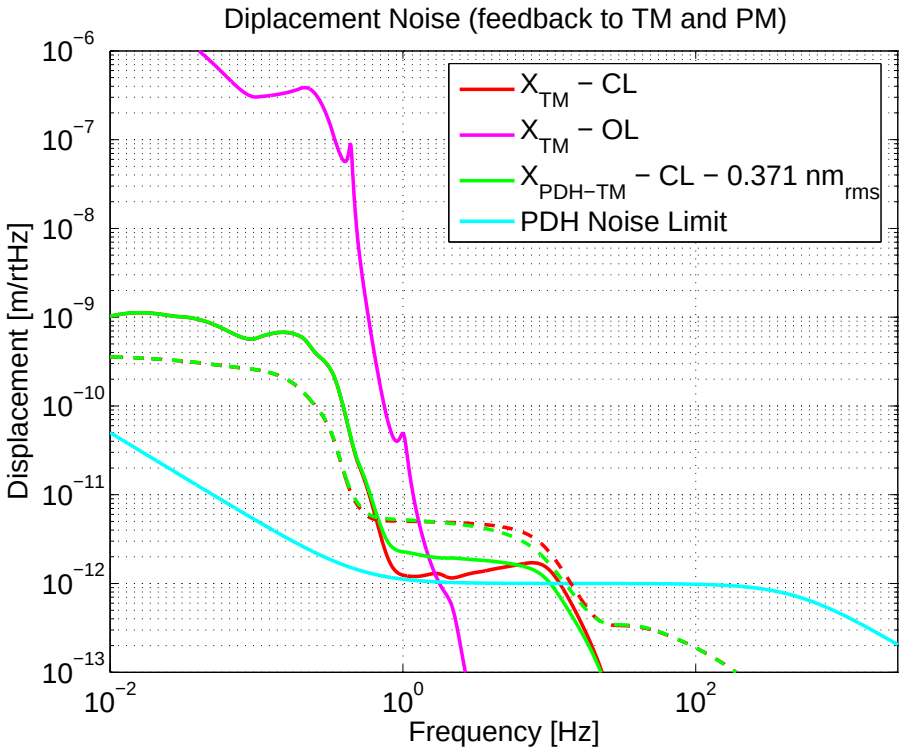

Figure 1: Open-loop and close-loop test mass RMS displacement.

4 System Overview

The single arm ALS system can be divided in to four sections: 1) test mass coating modifications, 2) auxiliary laser table, 3) in-vacuum transmon table and 4) end-station phase reference. There sections are shown in figure 2, which provides a system overview.

4.1 Test Mass Coating Modifications

The high performance coating for 1064 nm on the test masses will be modified to include a deterministic reflectivity at 532 nm. The ITM will have a high reflectivity of $> 99\%$, while

Table 1: ALS system requirements and parameters.

ITM HR@532 nm	$> 99\%$
ETM HR@532 nm	95%
Arm cavity Finesse (@532 nm)	~ 100
Frequency Dynamic range	± 20 kHz
Displacement noise	1 pm$\sqrt{\text{Hz}}$
Sensor Noise Limit	~ 70 mHz/$\sqrt{\text{Hz}}$
Phase Noise Limit	~ 70 mrad/$\sqrt{\text{Hz}}$ ($1/f$@ 1 Hz)

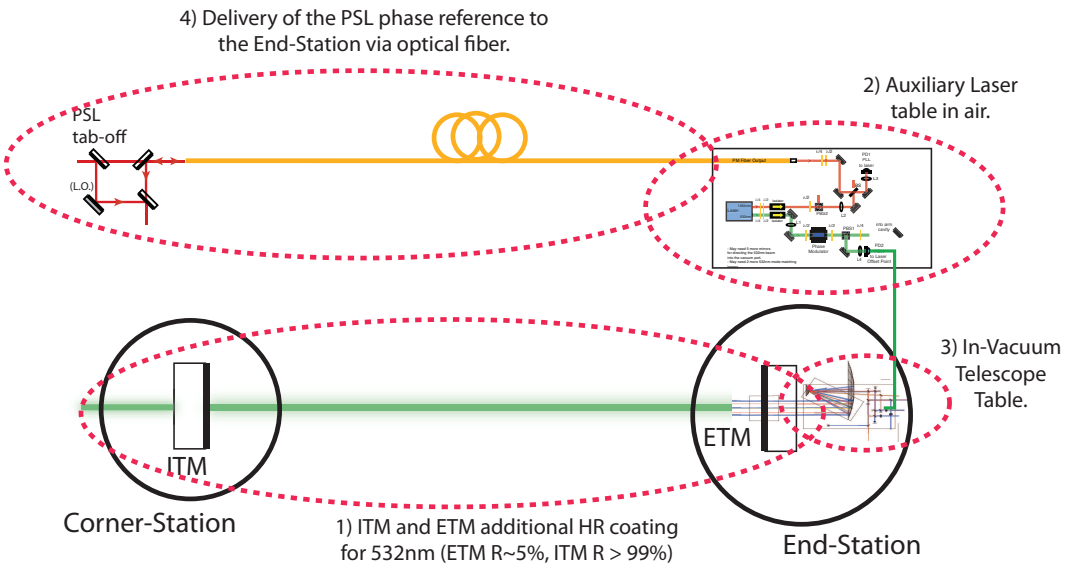

Figure 2: General overview of the Arm Length Stabilisation system.

the ETM will have a reflectivity of $\sim 95\%$. With these reflectivities, the cavity finesse will be $\sim$100. This has been included in the test mass coating specifications E0900068-v1 (ETM) and E09xxxxx (ITM).

4.2 Auxiliary Laser Table

The Auxiliary Laser Table is the optical table located next to the vacuum tank in the end-station, onto which the 1064/532 nm laser and accompanied optical injection components are mounted. Details of the optical layout and required components will be discussed in section 5.

The optical table will need to be large enough to hold a periscope to deliver the prepared beam into the vacuum. Depending on the separation of the BSC tanks at Hanford, only one table may be needed, onto which both auxiliary lasers are mounted.

4.3 In-Vacuum Transmon-Table

The Transmon Table is a suspended table behind the ETM quad suspension and holds the ETM Telescope[]. The table is approximately 23" x 40" (600 mm x 1000 mm), and is suspended from the BSC ISI platform. The suspension resonances are damped using eddy-current damping. This suspension system is currently in its early stages[].

The ETM telescope is a perfect 10:1 ratio beam reducer. Also on the table is a QPD for the ETM transmitted beam, onto which the image of the ETM HR coating is projected. This makes the QPD insensitive to the motion of the table. Also on the table are the DC alignment QPD for the ALS system and Hartmann pick-off.

More details and the optical layout are discussed in section 6

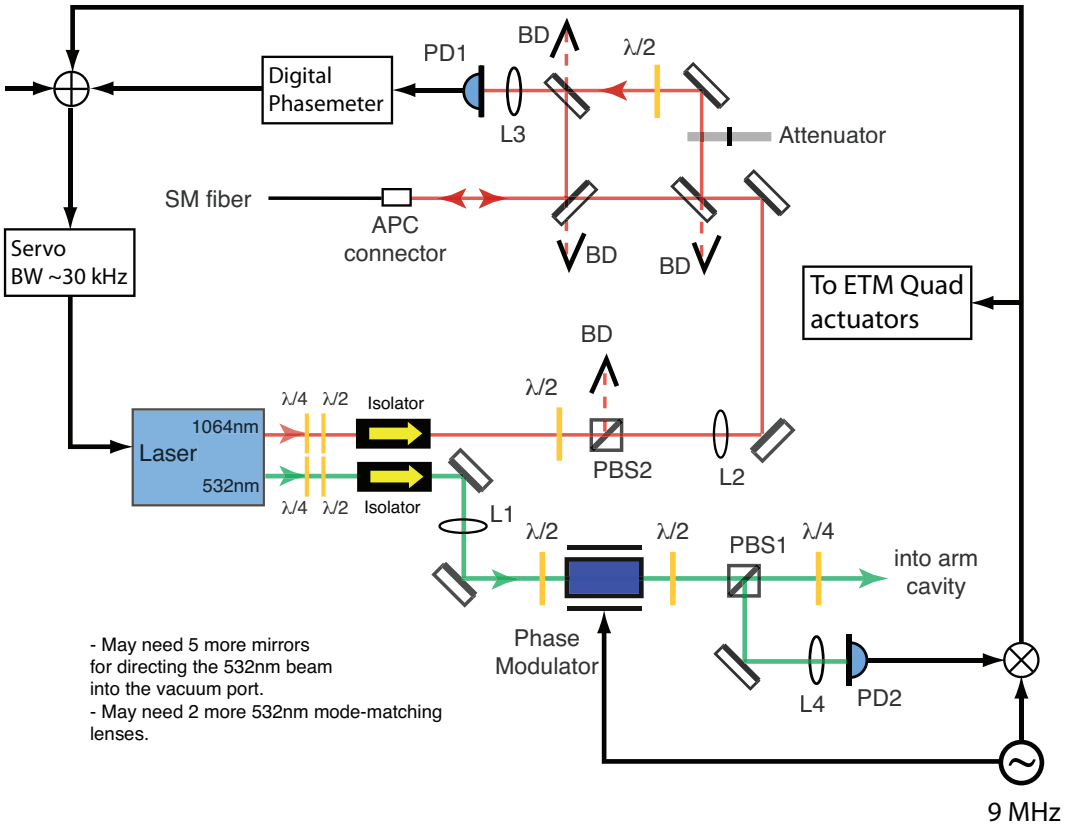

Figure 3: Layout of the end-station laser table. The laser is stabilised to the fiber output using the 1064 nm beam, and feedback is to the laser actuators (PZT and temperature). The 532 nm laser output is mode-matched and locked to the arm cavity, by feeding back to the offset point of the 1064 nm feedback servo. The high gain LSC detectors of the ETM transmitted beam used in the full IFO acquisition process are not shown.

4.4 End-Station Phase Reference

The auxiliary laser needs to be phase locked to the main pre-stabilised laser (PSL) in the corner station. This is required so during the full IFO acquisition when the cavity offset is reduced the arm cavity is not jittering around the offset point. To do this, a small amount of power is picked off from the PSL and sent to the station using an optical fiber. The fiber output is then combined with 1064 nm output of the auxiliary laser to generate a heterodyne beatnote. This beatnote is then used to phase lock the auxiliary laser to the PSL. Unfortunately, the fiber will introduce additional phase noise which will dominate the phase locking stability. An additional control system needs to be implemented to cancel out this fiber phase noise, this will be described in more detail in section 7.

5 Auxiliary Laser Table

The laser table holds the auxiliary dual wavelength laser (532 nm/1064 nm), the 532 nm injection optics and the 1064 nm fiber phase noise cancellation optics. The 1064 nm beam is

used to phase lock the laser to the phase reference delivered by the optical fiber, while the 532 nm beam is used to stabilise the arm cavity, using the standard PDH technique.

The 1064 nm output has the standard beam preparation (wave plates and faraday isolator). This output has ∼1 W of optical power, so a half-wave plate and polarising beam splitter are installed to provide some control of the optical power. The unused power is directed onto a high power beam dump. The power control is adjustable so that approximately 1 mW of power is injected into the fiber. An additional attenuator for the local oscillator beam is used so the RF output of PD1 does not saturate. A half waveplate provides the means to optimise the heterodyne beatnote. More details about the fiber noise cancellation is given in section 7.

The 532 nm beam is prepared with phase modulation sidebands (9 MHz), for the PDH readout, and injected into the arm cavity, via the ETM Transmon table. The PDH readout is used to initially feedback to the laser frequency, using PD2. This can be done in various ways, using an AOM or feeding back to the laser PZT. Because the fiber noise stabilisation is the high bandwidth feedback loop it is proposed to add the PDH feedback signal to the offset point of the fiber noise cancellation servo.

The vacuum viewport, where the 532 nm beam enters the vacuum, is located high so a periscope is required to guide the beam from the table into the viewport. Alternatively the table can be placed on tall piers to remove the need for a periscope.

Also on the table are the high-gain LSC detectors used to aid in the lock acquisition of the arm cavities with the corner cavities.

5.1 Frequency Range

The dynamic range is dominated by the displacement at low frequency $\sim 0.3\ \mu\mathrm{m}/\sqrt{\mathrm{Hz}}$ at 0.2 Hz (see figure 1). The dynamic range frequency requirement is,

$$\delta x_{0.2\,\mathrm{Hz}} \approx 3 \times 10^{-7}\ \mathrm{m}\sqrt{\mathrm{Hz}} \tag{1}$$

$$\Delta\nu = \frac{\delta x\, c}{\lambda\, L} = \frac{3 \times 10^{-7} \cdot 3 \times 10^{8}}{532 \times 10^{-9} \cdot 4000} = \pm 20\ \mathrm{kHz} \tag{2}$$

This frequency range can easily be covered by feedback to the laser frequency (PZT and temperature), as shown in figure 4.

6 In-Vacuum Trans-Mon-Table

(parts are taken from Sam's 'ETM Transmitted Platform' document)

The in-vacuum ETM transmission monitor table, aka Transmon table, is located in vacuum behind the ETM quad suspension. Located on the transmon table the beam reducing telescope, an off-axis refractive telescope. The table is suspended from the BSC ISI platform

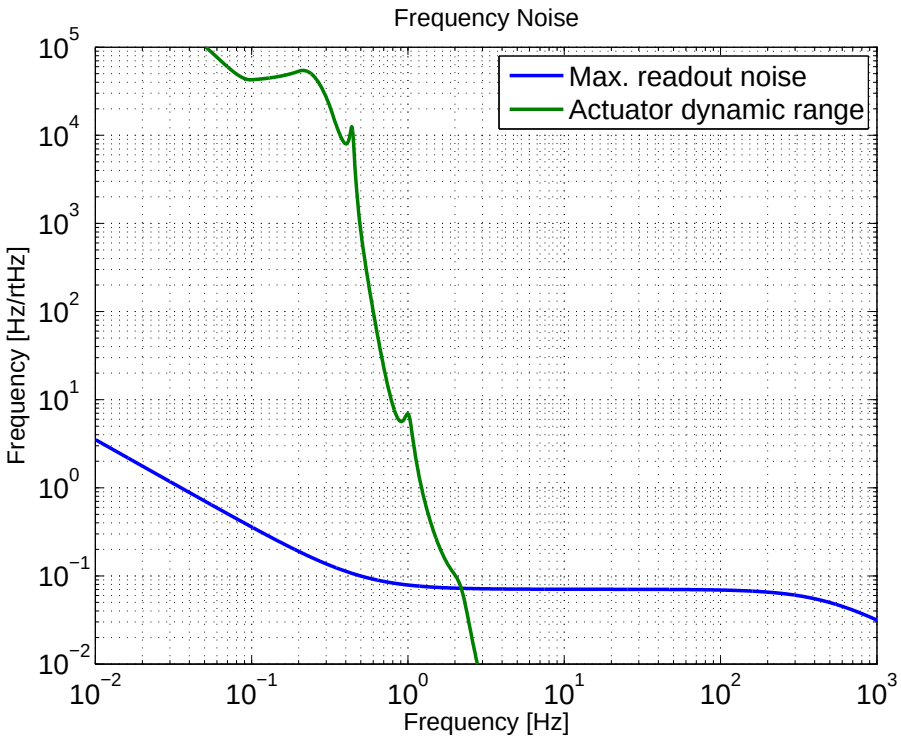

Figure 4: Dynamic range of the frequency actuator and the equivalent sensor noise.

such that the primary mirror of the beam reducing telescope is centered with the 1064 nm beam transmitted through the ETM. The design of the table suspension is TBD.

The transmon table is responsible for, in rough order of importance;

1. aligning the 1064 nm beam to the low-gain QPD which is located on the transmon table,
2. injecting the 532 nm auxiliary beam for arm length stabilisation during lock acquisition,
3. extracting the 532 nm beam from the vacuum during lock acquisition,
4. safely dumping the excess transmitted power,
5. preventing scattered light from influencing the interferometer,
6. delivering and extracting the 532 nm Hartmann beam.

There is an option to include 532 nm ASC quadrant detectors on the table. These will help with the ASC control of the full IFO. This needs further study.

The arm cavity will have a 6 cm beam waist ($1/e$ electric field radius) at the ETM. The 10:1 Beam Reducing Telescope (BRT) reduces the waist to 6 mm, small enough for transmission through 45-degree, 2-inch optics. The beam size is large compared to a 3 mm photodiode, so additional lensing is required for the in-vacuum sensors. However, the large IR beam size reduces the intensity incident on the in vacuum beam dumps which simplifies their design.

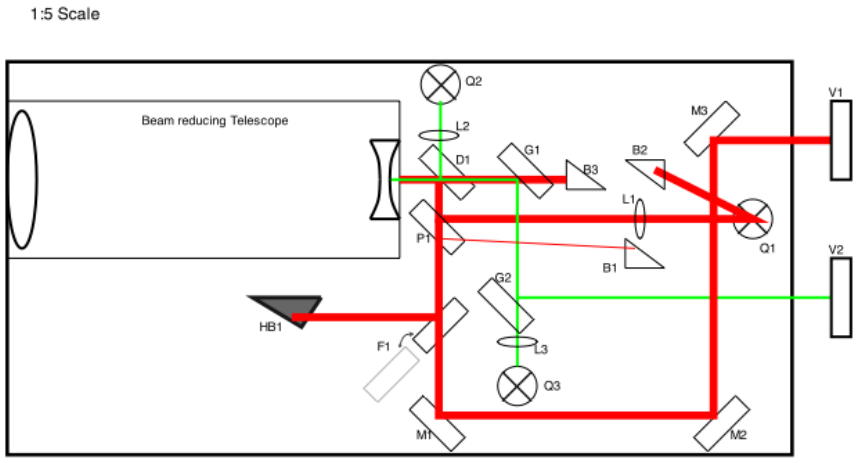

Figure 5: Schematic of the ETM transmission monitor table layout (SW).

Figure 5 shows a schematic layout of the Transmon table. Once the arm cavity is used in full IFO operation, approximately 5 W of optical power at 1064 nm is transmitted through the BRT (0.75 MW arm cavity power buildup and 5 ppm ETM transmission). There will be a 2% wedged mirror (P1) providing a pick off for the 1064 nm beam onto a QPD, used for beam centering and lock acquisition. During full IFO operation the 2% wedged mirror delivers ∼100 mW to the QPD. Ghost reflections from the 2% mirror and QPD are dumped on low power beam dump (B1). The remainder of the transmitted beam through the 2% wedge is guided of the table through a viewport outside the vacuum. This beam is used during lower power operations, to aide the lock acquisition of the arm cavity with the central cavities. During science mode, a shutter on the Transmon table prevents this beam from leaving the vacuum to prevent any back scatter and is directed to a high power beam dump HB1.

Prior the 2% wedged mirror there is a dichroic mirror (D1), which will reflect ∼99% of the 1064 nm beam and transmit the most of the 532 nm beam. Two mirror for the 532 nm beam (G1 and G2) will direct the 532 nm beam out of the vacuum through viewport (V2). Behind the steering mirror G1 (which is a second dichroic) is a 1064 nm beam dump (B3). The steering mirror G2 is partly transmissive to pass a small amount of 532 nm beam on to a QPD (Q3). The QPD Q3 senses the back reflected green light from the ETM for alignment of the 532 nm beam into the arm cavity. Similarly, the reflected path of D1 has lens L2 and QPD Q2 to sense the input alignment of the 532 nm beam. Finally, if too much 1064 nm light is transmitted through the green path, a Long Wave Pass dichroic filter or polariser can be placed between G2 and the viewport in order to reduce the 1064 nm transmission.

Currently the Transmon Table layout and suspension is being redesigned.

7 End-Station Phase Reference

To provide a smooth transition between the independent arm cavity locking using ALS and the full IFO lock acquisition, the auxiliary laser and the PSL need to be phase locked. The

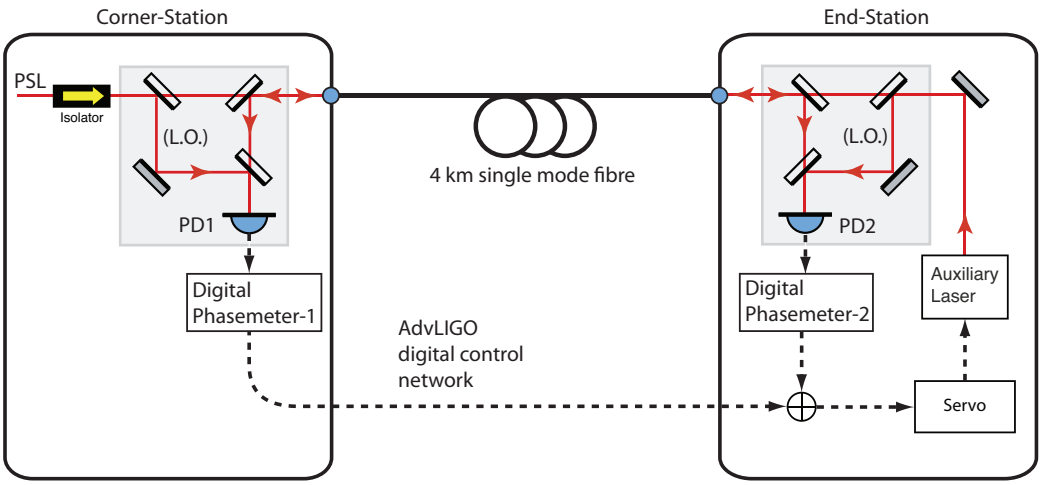

Figure 6: Layout of the fiber induced phase noise cancellation scheme.

required frequency stability is <0.1 Hz/$\sqrt{\text{Hz}}$ up to 100 Hz (see T0900095). To achieve this, a pick off beam from the PSL is sent to the end station using a single mode optical fiber. The output of this fiber in the end-station is then used to create a heterodyne beatnote with the 1064 nm beam from the auxiliary laser. This beatnote is then used to phase lock the two laser together. Unfortunately the 4 km long fiber will introduce phase noise due to temperature drifts and acoustic pickup. The fiber induced phase noise dominates the phase locking performance in the end-station. An additional control loop needs to be installed to suppress the fiber phase noise.

In the proposed baseline design two digital phasemeters are used to cancel the fiber phase noise. In addition the technique using two AOMs is used as a backup (see appendix A). Figure 6 shows the principle layout for the fiber phase noise cancellation scheme. The figure shows the layout for a single arm, and will need to be duplicated for the second arm. The faraday isolator (top left in figure 6) is used to prevent any reflections due to the coupling of the free space beam into the optical single mode fiber. It also prevents coupling of the end-station auxiliary laser from injecting into the PSL. All fiber connectors need to be angle-physical contact (APC) connectors to reduce any back reflections and residual interference. The optics and photodiodes are mounted onto a single breadboard for easy assembly and intergration. The two breadboards in the corner-staiotn are placed on the PSL table. The two breadboards can be stacked (or combined) if there is limited real-estate on the PSL table.

The heterodyne beatnote in the end-station is recorded on PD2 and RF signal is connected to a digital phasemeter. The digital phasemeter is implemented on a Field Programmable Gate Array (FPGA) in which all demodulation is done digitally. Using this approach the phase of the beatnote can be tracked over many cycles, and the offset frequency can be chosen/determine on the fly. The phasemeter output is injected into the locking servo which provides the feedback signal to the PZT and temperature actuators of the laser. This also can be implemented on the FPGA. This locking loop locks the PSL and auxiliary laser together, excessive fiber induced phase noise is still present and is injected on to the auxiliary laser frequency.

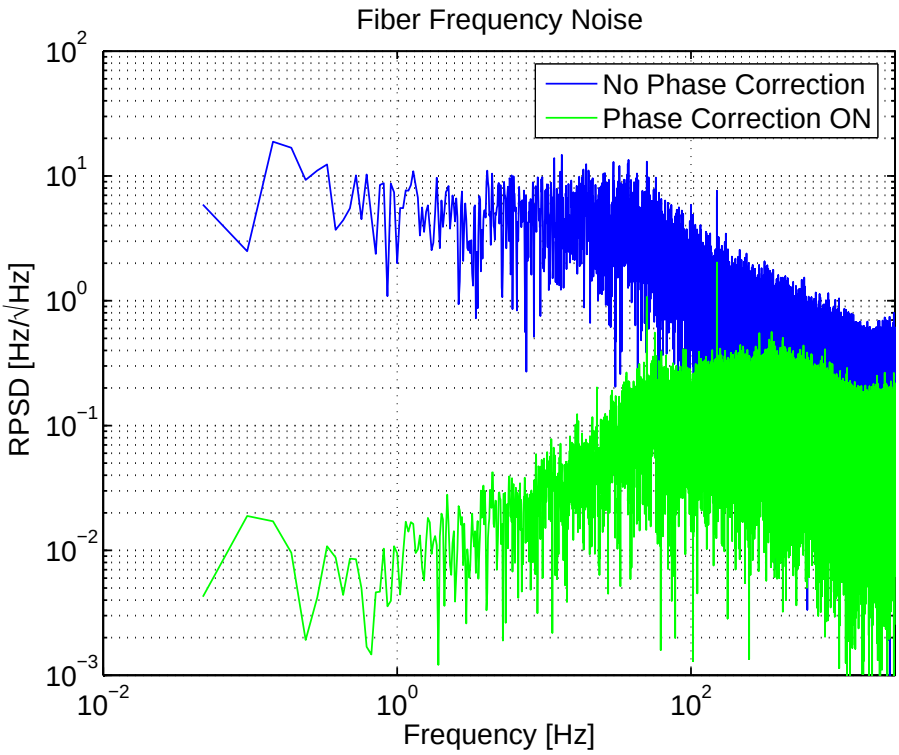

Figure 7: Fiber noise suppression results from using the counter propagating beam approach. A 10 km single mode fiber is used in the test, with 1 mW injected into the fiber at both ends. The heterodyne beatnote was at 6.13 MHz (on both detectors) and the phase fluctuations measured using the digital phasemeter. Both traces are measured on an out-of-loop detector, the blue (top) trace is a representation of the single pass fiber induced phase noise. While the green (lower) trace shows the out-of-loop fiber phase noise suppression.

To cancel the fiber induced phase noise, the auxiliary laser is injected into the optical fiber and sent to the corner-station. Here a second heterodyne beatnote is recorded on photodiode PD1 (at the same frequency as on PD2). A second phasemeter is used to measure the phase fluctuations of the beatnote, which represents the fiber induced phase noise. This phasemeter is located on an FPGA as well. The phase fluctuations are sent back to the end-station (via the CDS network, or a single CAT-6 ethernet link) and added prior the locking servo. This will cancel the fiber induced phase noise, with some initial results shown in figure 7.

Any polarisation drift due to the fiber will result in a drift of the amplitude of the heterodyne beatnote. The digital phasemeter can easily handle these amplitude changes, as it has a dynamic range of few orders of magnitude.

7.1 Key Hardware

The two RF photodiodes are ac coupled with a bandwidth of ∼100 MHz (e.g. New Focus 1811). Each detector is connected to a high speed ADC (Maxim 19588evkit), which in turn is connected to the FPGA via a 96-pin digital connector. The FPGAs (National Instru-

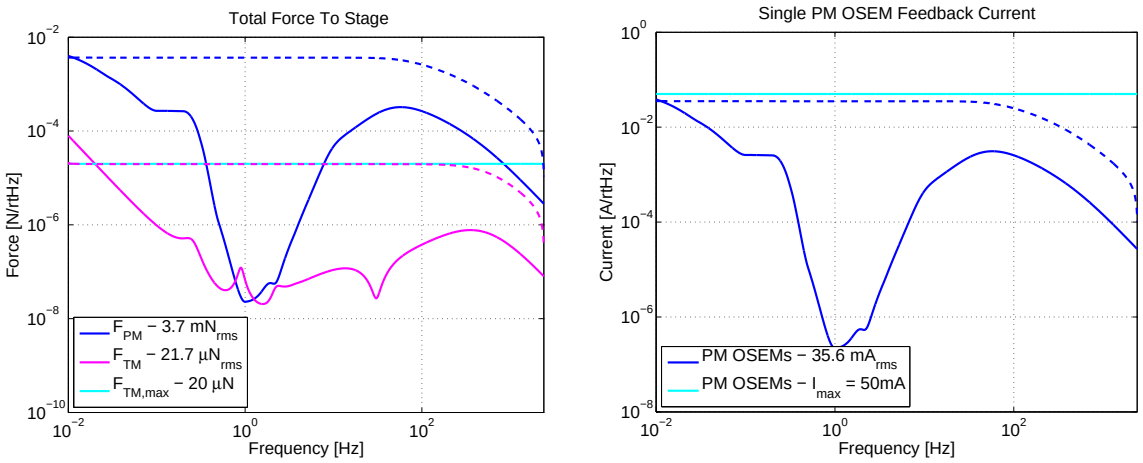

(a) Force amplitude spectrum to the test mass and the penultimate mass.

(b) Single OSEM feedback current.

Figure 8: Feedback to the penultimate mass and test mass. The dotted lines represent the rms values.

ments PXI-7853R) for the two phasemeters are located inside a PXI chassis, one for each phasemeter. The FPGA in the end-station is the master controller and provides feedback to the auxiliary laser (PZT and temperature) using its built-in DAC channels. The phasemeter output from the corner station is transferred using a $1 - 10$ kHz signal link (CAT-6, or equivalent) between the chassis. To lock the laser frequency to the arm length, the PDH error signal will be injected into the FPGA and summed with the phase noise cancellation signal. The error signal to the FPGA can be provided in analog or digital form.

In each chassis there will be a real-time controller, which communicates and transfers data from the FPGAs. The chassis in the corner station can hold both FPGAs for the phasemeter for either arm. A PC running Windows and LabView will be used as a host for the control and program environment for the FPGAs. A LabView EPICS daemon, running on the host, will communicate control signals between the FPGAs and the LIGO CDS.

8 Lock Acquisition

Initially, the auxiliary laser will be phase locked to the PSL using the beam delivered by the optical fiber. This feedback loop will have an approximate locking bandwidth of ∼35 kHz.

The error signal from the demodulated PDH sidebands is fed back to the laser frequency to lock the laser to the arm length fluctuations. The required frequency dynamic range is $\sim$ 20 kHz (see T0900095), which the laser can quite easily follow but may be limited by the fiber noise cancellation servo loop. Once the laser is locked to the arm cavity length fluctuations, the PDH error signal is in its linear range and can be used to feedback to the ETM quad suspension. Feedback is provided to the penultimate mass (PM) and the test mass (TM). This has been modeled in Simulink with the results shown in figure 1.

The arm length stabilisation performance is limited by the sensor noise and the maximum

feedback current and force of the quad actuators. The sensor noise is limited by the fiber phase noise cancellation performance. The sensor limit is set to the equivalent displacement of 10^{-12} m/$\sqrt{\text{Hz}}$, while the maximum PM OSEM current is set to 50 mA RMS and the ESD force to 20 μN RMS. These modeling results are shown in figure 1 with the actuator feedback signals in figure 8.

A Phase Reference - AOM approach

An alternative scheme to cancel the fiber induced phase noise is shown in figure 9 which include polarisation control. This method is to be tested at the LIGO 40m lab. The main difference is that the 40m lab is using polarisation maintaining fiber, so the polarisation controller in the end-station is not necessary (for the 40m lab). Also, the fiber modulator and faraday mirror in the figure are shown as fiber components. They can be replaced with bulk components.

The two AOMs are used to decouple the two beams traveling in opposite directions in the fiber, and to create a beatnote frequency at a convenient RF frequency on PD1. This approach has been demonstrated by the JILA/NIST group [1, 2]. Also, AOM1 is used as the frequency actuator to cancel the fiber induced phase noise at the end-station. In the end-station, a faraday mirror which rotates the polarisation of the reflected light by 90°. Any polarisation fluctuations obtained in the first fiber pass will be cancelled in the return pass and is detected on PD1.

The faraday mirror lets ∼5% through, which will pass through a motorised half wave-plate set at 45° in respected to the following polarising beam splitter (PBS). The PBS will split the power 'equal' onto both photo detectors. The auxiliary beam has a half wave-plate as well, set at 45° in respect the the PBS. Two additional half wave-plates just in front of the two detectors will rotate both beam so they interfere and create a heterodyne beatnote on either detector.

To control any large polarisation drift ($< 45°$), the DC power on the two detectors are subtracted and used as a control signal to the motorised rotation stage to keep the beam splitting ratio close to 50/50. The two heterodyne beatnotes out of the two detectors are used to phase lock the auxiliary laser to the PSL.

References

[1] P. A. Williams, W. C. Swann, and N. R. Newbury. High-stability transfer of an optical frequency over long fiber-optic links. *J. Opt. Soc. Am. B*, 25(8):1284–1293, 2008.

[2] Seth M. Foreman, Kevin W. Holman, Darren D. Hudson, David J. Jones, and Jun Ye. Remote transfer of ultrastable frequency references via fiber networks. *Review of Scientific Instruments*, 78(2):021101, 2007.

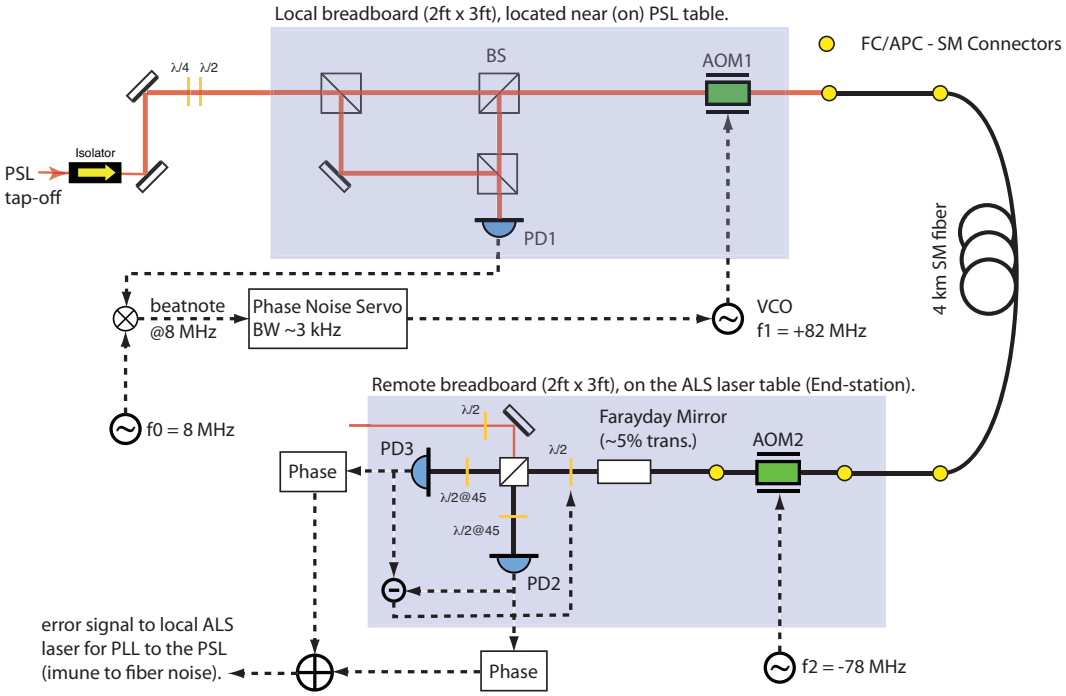

Figure 9: Layout of the fiber induced phase noise cancellation scheme using frequency shifting to obtain the heterodyne beatnote.